hydrology

MDPI

Article

Spatial–Temporal Response of Urban Flooding to Land Use Change: A Case Study of Wuhan's Main Urban Area

Tianle Wang [1,2] and Yueling Wang [1,3,*]

[1] Key Laboratory of Water Cycle and Related Land Surface Processes, Institute of Geographic Sciences and Natural Resources Research, Chinese Academy of Sciences, Beijing 100101, China; wangtianle23@mails.ucas.ac.cn
[2] University of Chinese Academy of Sciences, Beijing 100049, China
[3] Key Laboratory of Compound and Chained Natural Hazards, Ministry of Emergency Management, Beijing 100085, China
* Correspondence: wangyl@igsnrr.ac.cn

Abstract

Against the backdrop of rapid urbanization and an increase in extreme rainfall, the impermeable expansion caused by land use changes is significantly altering the urban property convergence process and intensifying the risk of waterlogging. To reveal the impact of land use change on the urban flooding processes, this study takes the main urban area of Wuhan (MUAW) as an example. Based on land use data from 2006 and 2020, it designs rainfall events with return periods of 5, 50, and 100 years. The NewFlood two-dimensional hydrodynamic model is employed to simulate flood evolution, with results validated against flood-prone locations. Flow velocity changes at typical flood-prone points are grouped and statistically analyzed according to land use conversion types. The results showed the following: (1) Between 2006 and 2020, land use transfer in MUAW is primarily influenced by urban sprawl and cropland reduction. (2) Urban expansion led to an increase in the area and depth of rainwater accumulation during rainstorms, which was highly aligned with the direction of urban sprawl, thereby increasing the risk of urban flooding during rainstorms. (3) Land use transfer has a limited impact on the maximum water depth and flow direction in MUAW. However, it can increase peak flow velocity or shift the peak time earlier, reducing the city's available emergency response time and increasing the difficulty of emergency response. The contribution of this paper lies in quantifying the waterlogging effect of land use change from dynamic dimensions such as "flow velocity—peak occurrence time", providing process evidence for the assessment of urban early warning advance, the allocation of drainage capacity and land use control, and offering a reference for prioritizing the layout of nature-based solutions and green infrastructure in low-lying catchment areas and key catchment channels to reduce flood risks.

Keywords: land use change; urban flooding; NewFlood model; main urban area of Wuhan

Check for updates

Academic Editor: Andrea Petroselli

Received: 20 November 2025
Revised: 16 December 2025
Accepted: 19 December 2025
Published: 22 December 2025

Copyright: © 2025 by the authors. Licensee MDPI, Basel, Switzerland. This article is an open access article distributed under the terms and conditions of the Creative Commons Attribution (CC BY) license.

1. Introduction

In recent years, global climate change and urbanization have jointly exacerbated urban flooding [1,2], threatening sustainable urban development. The rapid expansion of cities leads to changes in land use, increases the surface runoff process and hydrological response mechanism [3], resulting in shortened runoff time and increased rainfall peak, thereby significantly increasing the risk of urban flooding. Frequent extreme rainfall events have also increased the burden on urban drainage systems [4,5], posing a severe challenge to urban

rainwater management and flood control and disaster reduction. Therefore, analyzing the impact of land use change on the urban flood process is helpful for understanding the evolution law of urban rainwater and providing support for building resilient cities. At present, many scholars adopt various methods to explore the impact of land use change on urban flooding. Based on the simulation mechanism, the relevant models can be divided into two categories. One type of research mainly relies on hydrological mechanism, focusing on quantifying runoff generation and catchment processes and runoff response analysis, including SCS-CN, SWMM, SWAT, L-THIA, InfoWorks ICM and Wallingford model [6]. For example, Ma et al. [7] studied the regional runoff characteristics of Zhengzhou based on SCS-CN model. Zhao et al. [8] evaluated the ecological health of Yangmei River Basin Based on landscape model and SWMM model. Another kind of research focuses on hydrodynamic mechanism, emphasizing the detailed characteristics of flood evolution and surface hydrodynamic process. The models used include Mike Flood, XPSWMM, LISFLOOD-FP and NewFlood [9]. For example, Yan and Lu et al. [10] used MIKE Flood model to simulate and analyze urban waterlogging and river overflow in the south section of Fuhai River in Shenzhen. Wu et al. [11] constructed the XPSWMM model to explore the causes of urban waterlogging in the main urban areas on the South Bank of the Pujiang River. Despite existing research addressing urban waterlogging, a significant research gap persists in analyzing the dynamic response of surface runoff to land use change under natural hydrological conditions. Furthermore, the majority of prior studies have primarily relied on single rainfall events or static simulation periods, consequently failing to comprehensively reveal the dynamic impact of land use change on urban waterlogging across various rainfall return periods. We contend that the exclusive reliance on single-event and static-period analyses is insufficient for a robust and comprehensive assessment of the hydrological influence of land use change. This viewpoint is supported by recent literature (e.g., Pelorosso et al. [12]). Therefore, in-depth analysis of the land use change's dynamic response to urban waterlogging across different rainfall return periods is critical. This will provide a novel research perspective for understanding the evolutionary mechanism of urban waterlogging and offer essential scientific support for optimizing urban spatial structure.

As the core area of the urban agglomeration in the middle reaches of the Yangtze River and a typical waterfront megacity [13], MUAW is flat and has many lakes. Due to the concentration and intensity of summer rainfall, MUAW has been facing a serious threat of urban waterlogging for a long time [14]. Furthermore, Wuhan is undergoing significant land use changes [15], characterized by rapid expansion of construction land and continuous reduction in cropland and water, making it a typical region for studying the impact of land use changes on urban flooding. Therefore, this study focuses on MUAW to explore the quantitative response between land use changes and urban flooding process, aiming to provide a reference for other rapidly urbanizing regions.

This study aims to reveal from the perspective of physical processes how the differences in hydrodynamic parameters caused by land use change (such as roughness/impermeability characteristics) affect the response of surface runoff convergence and urban waterlogging processes, with a focus on exploring the variation patterns of process indicators such as water depth, flow velocity, and peak occurrence time. Taking the MUAW as a case study, we employ high-resolution land use data (2006 and 2020) and multiple rainstorm scenarios (5 years, 50 years, and 100 years) to simulate the flooding process. For this analysis, we utilize the NewFlood hydrodynamic model, which is distinct from many existing models due to its superior stability and high computational efficiency crucial for large-scale, high-resolution urban simulation. NewFlood employs a Godunov scheme with simplified dry/wet boundary conditions for accurate simulation in complex terrain, while its high-performance parallel computing capability supports fine-scale grids,

significantly enhancing simulation speed and analytical precision. By simulating the natural flood process (excluding artificial drainage measures), this research quantitatively analyzes the impact of land use changes on water depth and flow velocity. The findings will provide a scientific basis for urban flood control planning and land use management, particularly for identifying potential flood-prone areas and optimizing the urban drainage network layout.

2. Materials and Methods

2.1. Study Area

Wuhan, a major city in the middle reaches of the Yangtze River, is located in a subtropical monsoon climate zone with abundant summer rainfall. Combined with its low-lying central area, urban flooding is particularly severe [16,17]. This study selected MUAW, including Jiangan, Jianghan, Qiaokou, Hanyang, Wuchang, Hongshan, and Qingshan (Figure 1), with a total area of 964 km^2. The relatively low-lying and flat terrain of MUAW, coupled with rapid economic development and high land use intensity, along with widespread gray infrastructure and hard underlying surfaces, makes this region particularly vulnerable to flooding disasters caused by torrential rains.

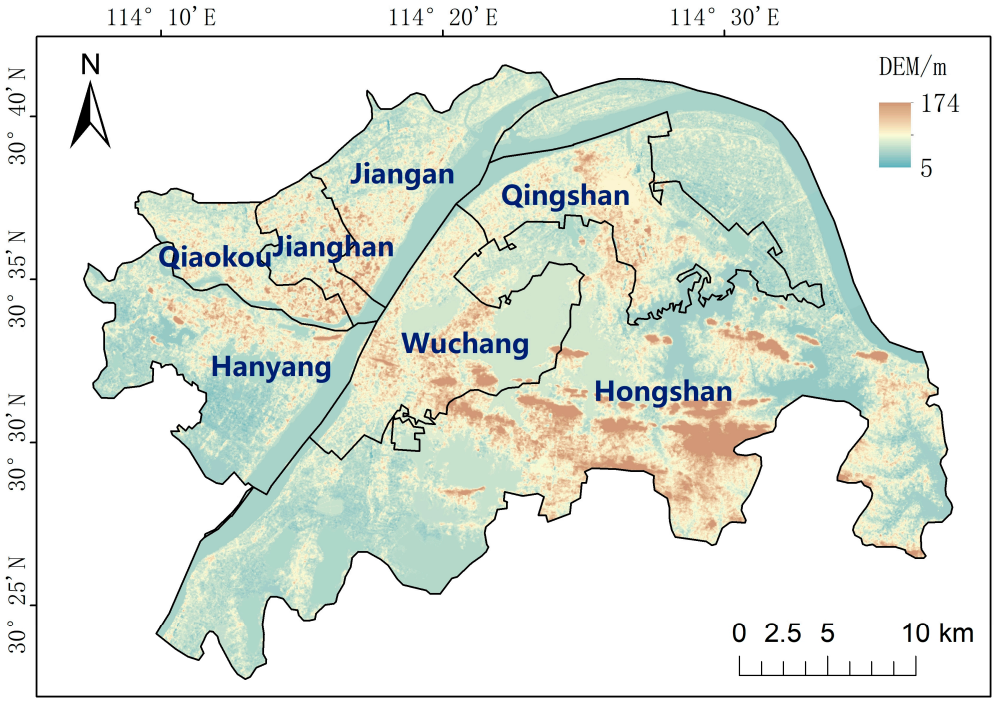


Figure 1. DEM of MUAW.

2.2. Methods

2.2.1. NewFlood Model

The NewFlood model is a fully two-dimensional hydrodynamic model based on a Cartesian uniform grid [18], with the main governing equations being the planar two-dimensional shallow water equations. The differential hyperbolic conservation form of the pre-equilibrium shallow water equations is as follows.

$$\frac{\partial q}{\partial t} + \frac{\partial f}{\partial x} + \frac{\partial G}{\partial y} = S \quad (1)$$

$$q = \begin{bmatrix} \eta \\ uh \\ vh \end{bmatrix}, F = \begin{bmatrix} uh \\ u^2h + \frac{1}{2}g(\eta^2 - 2\eta z_b) \\ uvh \end{bmatrix}, \quad G = \begin{bmatrix} vh \\ uvh \\ v^2h + \frac{1}{2}g(\eta^2 - 2\eta z_b) \end{bmatrix} \tag{2}$$

$$S = \begin{bmatrix} ss \\ -C_f u\sqrt{u^2+v^2} - g\eta\frac{\partial z_b}{\partial x} \\ -C_f v\sqrt{u^2+v^2} - g\eta\frac{\partial z_b}{\partial y} \end{bmatrix} \tag{3}$$

where t is time (s); x and y are Cartesian coordinates; η is water level (m); z_b is bed elevation (m); q is flow vector; f and G are flux vectors in the x and y directions, respectively; S is source term vector, including rainfall or infiltration source term ss, bottom slope source term and frictional source term; h is water depth (m); u and v are depth-averaged velocity components in the x and y directions (m/s); g is gravitational acceleration (9.81 m/s^2); C_f is the surface roughness coefficient; n is the Manning coefficient.

This study uses NewFlood hydrodynamic model, which shows excellent stability and efficiency in dealing with large-scale and high-precision urban flood simulation. Firstly, the advanced numerical core of NewFlood model can accurately and stably simulate the flood evolution process under complex urban terrain. The model uses two-dimensional finite volume Godunov scheme to solve the shallow water equation, and puts forward simplified boundary conditions for the common dry and wet boundary problems in urban environment, so as to maintain a good equilibrium solution. This enables the model to provide more stable simulation results when dealing with different flow patterns, which is very important for accurately characterizing the complex surface runoff caused by severe land use change. Secondly, considering the scale of this study, high-resolution land use data pose a major challenge to the computational efficiency of the model. The core advantage of NewFlood model lies in its excellent high-performance computing power. Using the powerful functions of modern parallel computing hardware, the model can quickly and accurately simulate complex flood dynamic processes [19]. This feature supports the use of high-resolution grids in this study, which can accurately capture the impact of land use change on flood path, discharge and inundation range, and significantly improve the authenticity of simulation and the accuracy of analysis. The validity of the model's application to the study area is evaluated by comparing simulation outcomes with historical observational data, the results of which are detailed in Section 3.1.

2.2.2. Roughness Coefficient

Roughness coefficient is a key link connecting surface characteristics and flood analysis [20]. The soil moisture in Wuhan is high and close to saturation, resulting in minimal infiltration effect. Therefore, the influence of the roughness coefficient on flood evolution is primarily considered in urban flooding simulation [21]. Roughness values are referenced from existing studies [22,23] and validated by the study [19], as shown in Table 1.

Table 1. Roughness coefficient of land use type.

Land Use Type	Roughness Coefficient
Impervious	0.016
Water	0.027
Grassland	0.030
Cropland	0.035
Forest	0.150
Barren	0.025

2.2.3. Land-Use Change Matrix

The land-use change matrix serves as a critical tool for analyzing the dynamic process of land use change. Unlike simple area statistics, this method quantitatively describes the direction and quantity of transfer between different land use categories during the study period [24,25]. By overlaying the land use maps from the beginning and the end of the period, the matrix reveals the internal conversion structure, identifying specific sources of newly added land types and the destinations of reduced land types. The formula is as follows:

$$S_{ij} = \begin{bmatrix} S_{11} & \cdots & S_{1n} \\ \vdots & \ddots & \vdots \\ S_{n1} & \cdots & S_{nn} \end{bmatrix} \quad (4)$$

where S represents the land area (km^2); n denotes the total number of land use types; i and j (i, j = 1, 2,..., n) represent the land use types at the initial time (2006) and the final time (2020), respectively. Specifically, S_{ij} represents the area transferred from land use type i to type j during the study period, effectively capturing the spatial evolution of land use in the MUAW.

2.3. Data Sources and Scenario Design

2.3.1. DEM and Land Use Data

The hydrodynamic simulation relies on high-precision underlying surface data. The Digital Elevation Model (DEM) with a spatial resolution of 30 m was obtained from the Geospatial Data Cloud Platform (http://www.gscloud.cn/) (12 December 2024) to characterize the terrain of the MUAW.

Land use data for 2006 and 2020 were derived from the CLCD dataset (https://doi.org/10.5281/zenodo.12779975) (24 December 2024), also with a 30 m spatial resolution. The importance of land use thematic resolution in environmental and hydrological evaluations has been emphasized in recent studies [26]. Accordingly, this dataset classifies the land cover into six distinct thematic categories relevant to urban runoff: impervious surfaces, water, cropland, forest, grassland, and barren land. This classification scheme corresponds to the roughness coefficients listed in Table 1. The selection of data from 2006 and 2020 corresponds to the implementation phase of the Wuhan City Land Use Master Plan (2006–2020), capturing the significant land surface transformations driven by rapid urbanization.

2.3.2. Rainfall Model and Scenario Design

To systematically analyze the impact of land use changes under varying stress conditions, this study designed a set of comparative simulation scenarios. The Chicago Design

Storm model was employed to synthesize rainfall events. The rainfall intensity (i) and average intensity (q) were calculated based on the local storm intensity formulas for Wuhan:

$$\dot{i} = \frac{9.686(1 + 0.887lgP)}{(t + 11.23)^{0.658}} \quad (5)$$

$$q = \frac{1614(1 + 0.887lgP)}{(t + 11.23)^{0.658}} \quad (6)$$

where i is the design rainfall intensity (mm/min); q is the design rainfall intensity (L/s·hm^2); P is the return period (years); t is the rainfall duration (min).

The study established six distinct simulation scenarios (Table 2) by combining the two land use scenarios (2006 and 2020) with three rainfall return periods (5-year, 50-year, and 100-year). The total rainfall duration was set to 180 min with a peak coefficient of 0.39. It is important to state that a spatially homogeneous rainfall event was simulated for the entire study area. While this approach effectively isolates the impact of land use changes by controlling meteorological variables, it simplifies the spatial variability of actual rainstorms. This assumption represents a limitation of the current study and points to a direction for future research involving spatially distributed rainfall radar data.

Table 2. Summary of simulation scenario design.

Scenario ID	Land Use Scenario	Rainfall Return Period (Years)	Description
S1	2006	5	Baseline land use under standard rainfall
S2	2006	50	Baseline land use under heavy rainfall
S3	2006	100	Baseline land use under extreme rainfall
S4	2020	5	Urbanized land use under standard rainfall
S5	2020	50	Urbanized land use under heavy rainfall
S6	2020	100	Urbanized land use under extreme rainfall

3. Results

3.1. Verification of the Simulation Results of Urban Flooding

According to data released by the Wuhan Water Affairs Bureau in 2020, Wuhan has a total of 59 flood-prone risk points, 46 of which are located within the study area. Building upon previous studies [27,28], this study integrates Wuhan urban flooding simulation in 2020 and employs a 2.5 m water depth threshold for analysis. The research findings indicate that 42 out of the 46 flood-prone locations highly coincide with the simulation results of this study (Figure 2), achieving a 91.3% overlap rate. The strong consistency between simulated outcomes and actual observational data fully validates the scientific rigor and reliability of the modeling approach employed in this research. Furthermore, the effectiveness of NewFlood model in urban flood inundation simulation has also been thoroughly validated in case studies of Wuhan by [19].

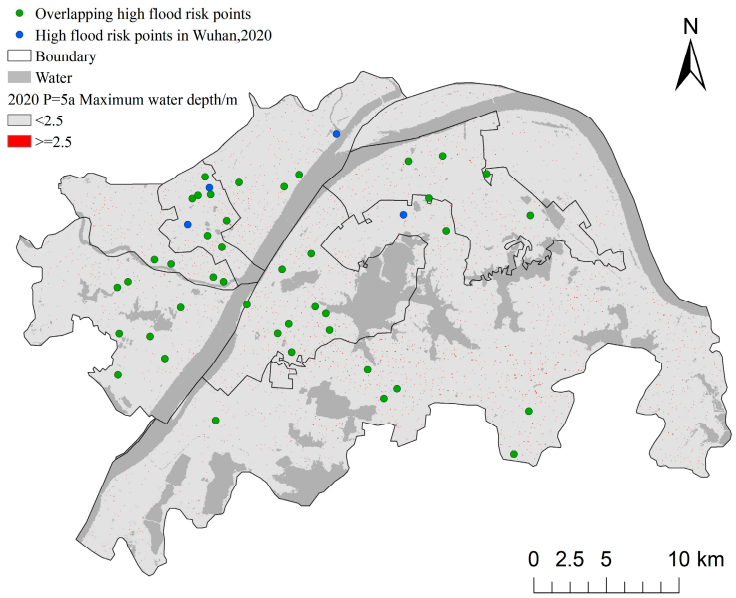


Figure 2. The results of model validation.

3.2. Characteristics of Land Use Change

3.2.1. Spatial Characteristics of Land Use Change

From 2006 to 2020, significant changes occur in land use within MUAW. Figure 3 shows the land use transformation map of MUAW, illustrating the spatial distribution of major land use shifts (transfer area greater than 1 km^2). Impervious in MUAW increases significantly, while cropland decreases significantly, and changes in water, forest, and grassland are relatively small. Except for Jianghan, land use in Jiangan, Qiaokou, Hanyang, Wuchang, Hongshan, and Qingshan all showed a shift from cropland to impervious and from water to cropland. The land use transformation in Hanyang and Hongshan is particularly significant, exhibiting not only diversity in land type changes but also a more pronounced degree of change.

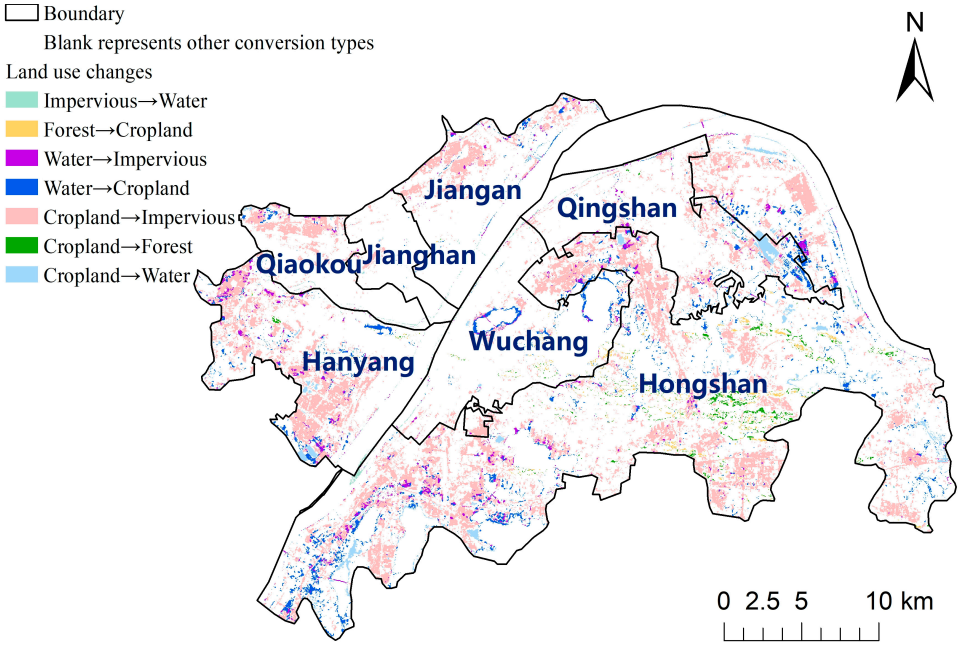


Figure 3. Land use transfer of MUAW from 2006 to 2020.

3.2.2. Analysis of Land Use Transfer

The land-use change matrix (Table 3) shows that from 2006 to 2020, the cropland in MUAW decreases by 113.43 km^2, with a change rate of −27.34%, mainly shifting to impervious (124.25 km^2), water (9.06 km^2), and forest (3.23 km^2). Impervious increases dramatically by 133.61 km^2, with a growth rate of 37.63%, primarily originating from cropland (124.25 km^2) and water (11.39 km^2). This is related to Wuhan becoming a central city in Central China in 2010, with the expansion of impervious meeting the demands of urbanization and rapid economic and social development. Water continues to decrease, mainly converted into cropland (19.46 km^2) and impervious (11.39 km^2). Although some areas have been converted from cropland to lakes, encroachment on water by lake reclamation and urban construction still exists, and water protection in MUAW remains a priority. Forest, as an important ecological land, decreases by 0.165 km^2, with the main conversions into and out of forests being cropland. The conversion amounts were basically balanced, indicating that MUAW has a strong awareness of forest resource protection during urban expansion. Grassland and bare land accounted for a very small proportion, decreasing by 0.24 km^2 and 0.03 km^2, respectively, showing minimal change.

Table 3. The land-use change matrix in MUAW (km^2).

Land Use Type		2020							
		Cropland	**Forest**	**Grassland**	**Water**	**Barren**	**Impervious**	**Total**	**Change Rate**
2006	Cropland	278.301	3.230	0.009	9.059	0.005	124.250	414.852	−27.343%
	Forest	3.270	14.356	0.000	0.016	0.000	0.115	17.757	−0.935%
	Grassland	0.030	0.000	0.000	0.000	0.002	0.216	0.248	−95.968%
	Water	19.455	0.005	0.000	170.275	0.01	11.387	201.133	−9.818%
	Barren	0.000	0.000	0.000	0.038	0.003	0.008	0.050	−62.000%
	Impervious	0.369	0.000	0.000	1.998	0.000	327.099	329.466	10.201%
	Total	301.425	17.591	0.010	181.385	0.019	463.074	963.505	-

3.3. The Influence of Land Use Changes on Water Depth in MUAW

Figure 4 shows that under rainfall scenarios with different return periods (5a, 50a, 100a), the area experiencing increased water depth rapidly expands during the initial rainfall phase (<70 min) as rainfall intensity rises, reaching its maximum at the peak moment (70 min) (5a: 227.1 km^2, 50a: 249.8 km^2, 100a: 256.3 km^2), and then tends to stabilize. This phenomenon is directly related to the time-varying characteristics of rainfall intensity. The rapid formation of surface runoff in the initial stage, coupled with the excessively high rainfall intensity during the peak period, led to a significant expansion of the flood-prone area. It is worth noting that with the extension of the recurrence period, the growth of the submerged area shows a non-linear decreasing trend (5 years → 50 years: +22.7 km^2; 50 years → 100 years: +6.5 km^2), indicating that the surface water storage capacity is approaching the critical value.

Figure 5 shows the spatial distribution of the increase in water depth at t = 70 min from 2006 to 2020 when the recurrence period of rainfall was 5 years. The areas with increased water depth are mainly concentrated in Hanyang, Wuchang and Hongshan districts. This is because the large lakes in Wuchang and Hongshan have a significant effect on water depth due to the influx of surface runoff, while densely urbanized areas such as Hanyang have a high proportion of impermeable surfaces, leading to a higher runoff coefficient, faster surface water accumulation, and localized sharp increases in water depth. Overall, the areas of increased water depth highly coincide with the direction of urban expansion, confirming the significant interference of land use change on flood evolution.

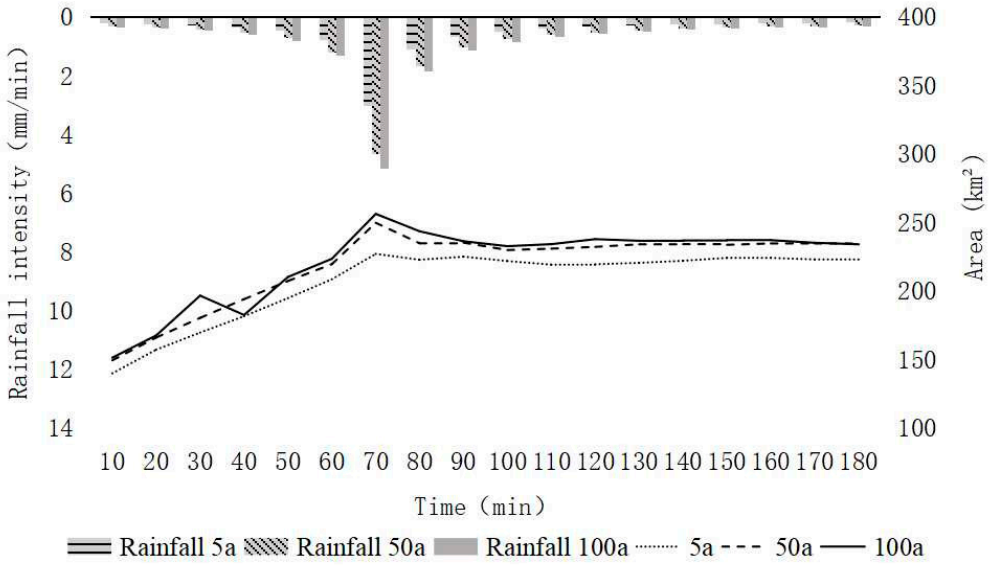


Figure 4. Variation in rainfall intensity between 2006 and 2020.

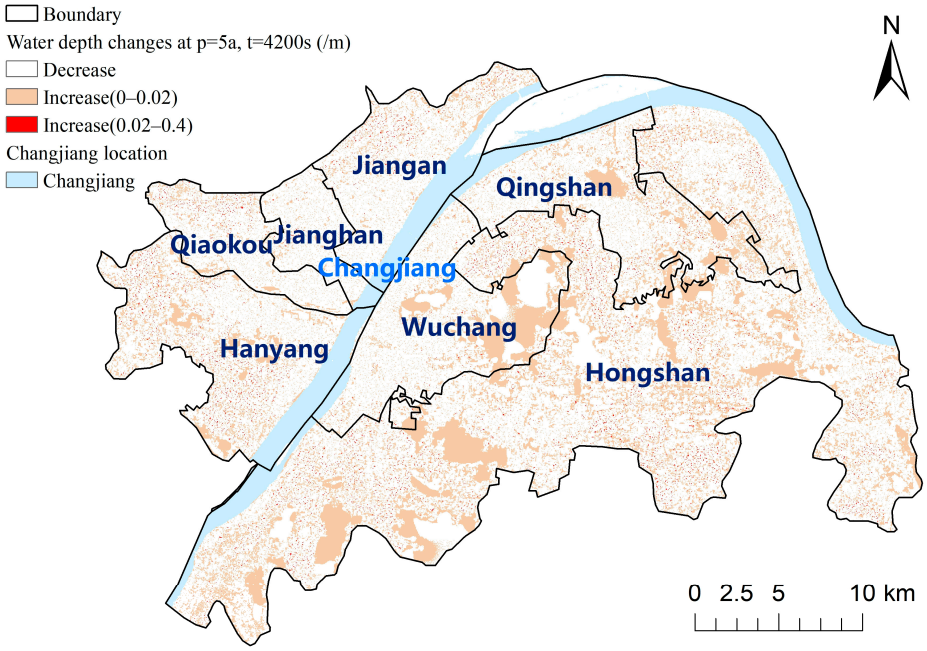


Figure 5. The spatial distribution of increased water depth.

3.4. The Influence of Land Use Changes on the Flow Velocity in Flood-Prone Areas

Based on the simulation results presented in Sections 3.1 and 3.2.1, and combined with authoritative data on flood-prone risk points released by the Wuhan Municipal Water Resources Bureau, this study selects eight flood-prone areas of concern with typical land use change characteristics. These areas cover different relocation types, including no change, water transforming into impervious, and cropland transforming into impervious. The specific locations are near Jianyi Road, near Yindun Street, Qinghua Overpass, Youyi Avenue Overpass, near the intersection of Baiyushan Qinghua Road and Kangning Road, near Xudong Avenue, near Luoshi North Road and Bayi Road, and near the intersection of Guanggu Fifth Road and Erquan Street (Figure 6). This study analyzed the impact of land use changes on the flow velocity in flood-prone areas by observing the flow velocity variations at these locations under different land use conditions.

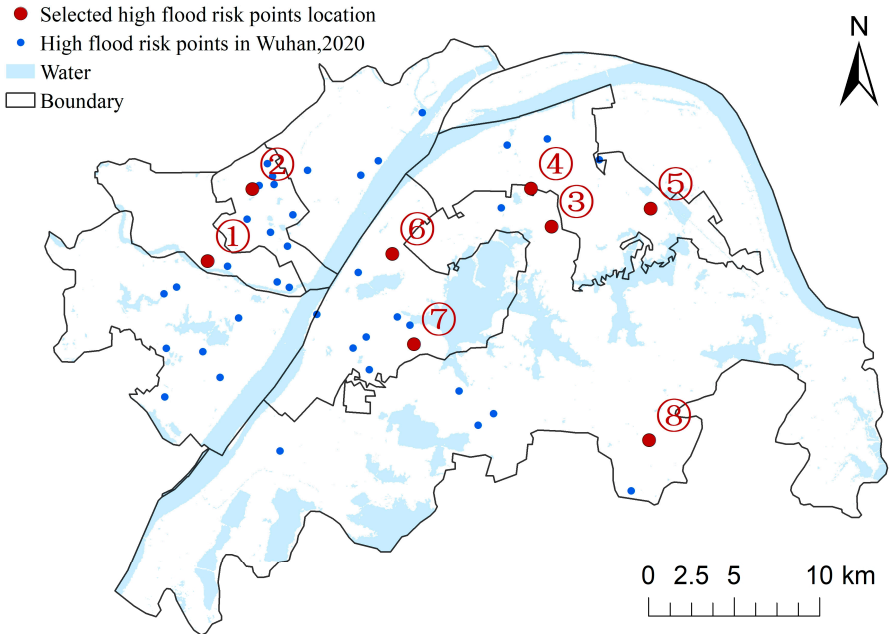


Figure 6. The location of the flood-prone area selected.

Figure 7 shows the variation law of flow velocity at flood detention points over time. The analysis of Table 4 illustrates the response of hydrodynamic parameters to land use dynamics. It is crucial to acknowledge that flow velocity and water depth at a specific location are influenced by the cumulative hydrological processes within the encompassing urban sub-basin. Consequently, land use changes in upstream or surrounding areas can alter runoff convergence and flow paths, potentially affecting a target location even if no land use changes occurred directly at that specific point between 2006 and 2020. In this study, although the land use types at points 1, 2, 3, and 6 remained unchanged, their hydrodynamic parameters were monitored for potential systemic impacts. The results indicate that these specific points experienced no significant changes in flow velocity and water depth, suggesting a relatively stable catchment environment. On the contrary, points 5, 7 and 8 changed from cropland to impermeable surface, while point 4 changed from water body to impermeable surface, resulting in a significant change in flow velocity. Specifically, the maximum flow velocities at flood control points 4 and 7 increased by 2.331 m/s and 6.345 m/s, respectively. At Points 5 and 8, the appearance time of the flood peak was advanced by 3 min and 2 min, respectively, and the maximum flow velocity increased by 1.920 m/s and 5.971 m/s, respectively. Regarding water depth variations, the maximum water depth changes at all flood-prone points are relatively consistent.

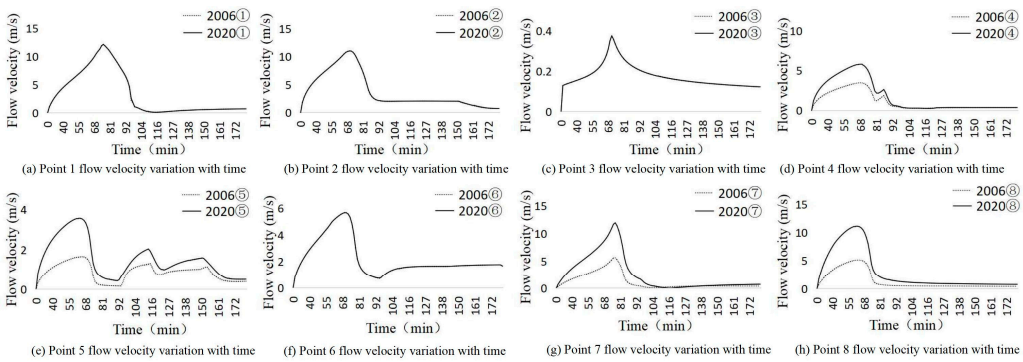


Figure 7. The flow velocity at flood-prone areas varies with time.

Table 4. Comparison of flow velocity and water depth results in flood-prone areas.

No.	Flood-Prone Location	Land Use Change (2006~2020)	Maximum Flow Velocity (m/s)			Time of Maximum Flow Velocity (min)			Maximum Water Depth (m)		
			2006	2020	Δv	2006	2020	Δv	2006	2020	Δv
1	Near Jianyi Road	No change	12.121	12.125	+0.004	75	75	0	4.495	4.496	+0.001
2	Near Yinhu Street	No change	10.993	10.992	0.000	70	70	0	4.256	4.256	0.000
3	Qingliuzi Interchange	No change	0.374	0.374	0.000	71	71	0	0.004	0.004	0.000
4	Youyi Avenue Overpass	Cropland converted to impervious	3.468	5.799	+2.331	68	68	0	4.344	4.344	0.000
5	Near Baiyu Chemical Plant and Kangning Road	Cropland converted to impervious	1.646	3.566	+1.920	66	63	−3	4.274	4.288	+0.014
6	Near Xuhong Avenue	No change	5.663	5.664	+0.001	70	70	0	4.019	4.020	+0.001
7	Raoyang Road and Bayi Road	Cropland converted to impervious	5.585	11.930	+6.345	77	77	0	4.570	4.570	0.000
8	Guanggu Third Road and Erquan Street	Cropland converted to impervious	5.124	11.095	+5.971	64	62	−2	4.358	4.371	+0.013

Land use change (transforming cropland or water areas into impervious surfaces) reduces surface roughness and accelerates stormwater runoff, leading to an increase in peak flow velocity and an earlier onset of the flood peak. Although its influence on the maximum water depth is limited, the impact on flow velocity is significant. To further quantify the flood disaster risk by integrating flow velocity and water depth, the Flood Hazard Rating widely adopted in the UK was employed as the evaluation indicator. The functional expression is defined as follows:

$$HR = d(v + 0.5) + DF \quad (7)$$

where HR denotes the hazard rating; d is the water depth (m); v is the flow velocity (m/s); and DF represents the debris factor.

To simplify the calculation, DF is set to 1 in this study [29], consistent with guidelines for water depths exceeding 0.25 m. By calculating the flood hazard rating [29], the flood risks at flood prone points 4, 5, 7, and 8 were found to increase by 45.53%, 43.57%, 96.51%, and 81.55%, respectively. These results confirm that the increase in flow velocity significantly escalates the risk of casualties and acts as a primary driver of urban flood risk.

The results of this study show that different types of land use conversion have different influences on the dynamic process of urban flooding. Compared with the points where land use remained unchanged, when cultivated land and water areas were transformed into impervious water surfaces, the peak flow velocity at typical points generally showed an increasing trend, and the peak flow velocity time at some points was advanced (Figure 7). In addition, the variation range of the maximum water accumulation depth at each point is relatively limited, and the overall difference in the maximum water depth under different scenarios is smaller than the variation range of the flow velocity index (Table 4). In conclusion, the impact of land use change on the process of urban flooding is more significantly

reflected in dynamic indicators such as flow velocity and peak occurrence time, while its influence on the maximum water depth is relatively weak.

Different flood-prone points exhibit varying flow velocity changes influenced by land use. Since the peak flow velocity at Points 7 and 8 occurs around 70 min, this critical time point is selected for plotting the flow field diagram (Figures 8 and 9).

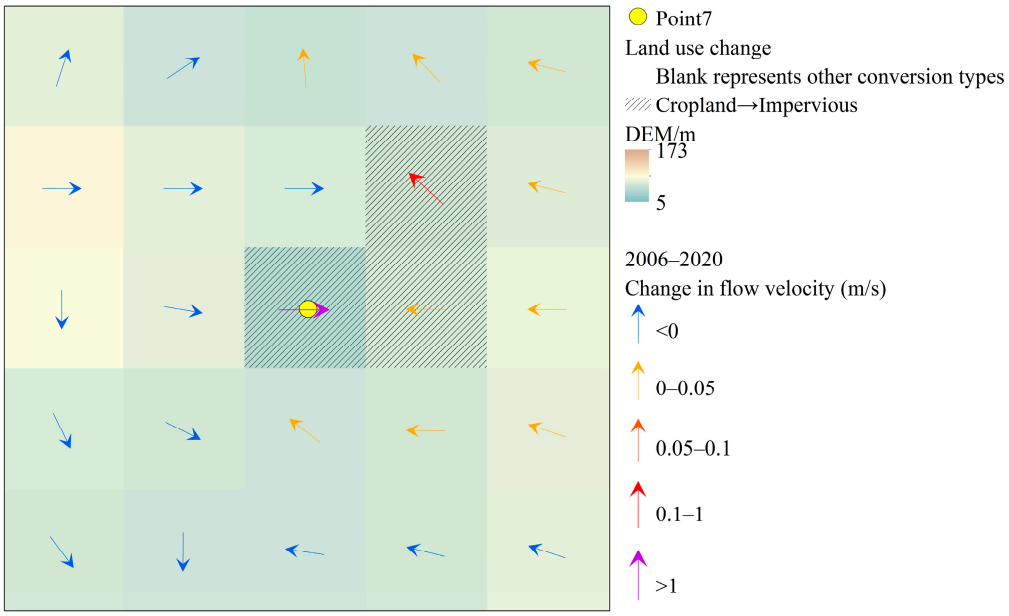


Figure 8. Flow velocity changes at flood-prone points 7.

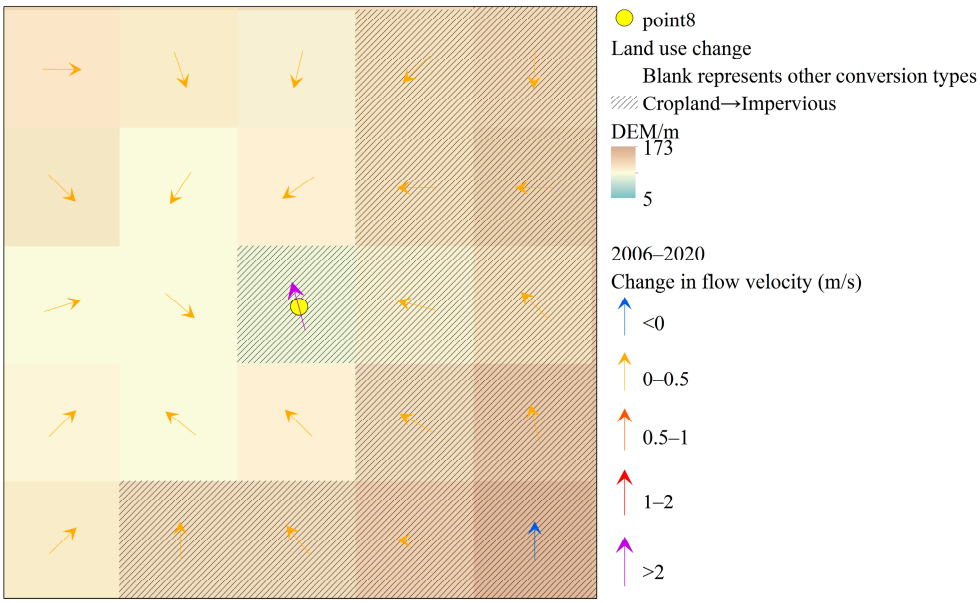


Figure 9. Flow velocity changes at flood-prone points 8.

Flood-prone point 7 is situated in a low-lying area northeast of MUAW. After the surrounding cropland is converted to impervious, flow velocity increased, but the flow velocity on the higher ground to the left decreased, although the overall peak flow velocity increased. Flood-prone point 8 is situated in a low-lying area where precipitation convergence significantly increases peak flow velocity. Surrounding flow velocities also rise, causing the peak flow timing to advance. Due to the combined influence of surrounding topography and land use changes, alterations in land use usually leads to an increase in

flow velocity or an earlier appearance of flood peaks, and these two phenomena often occur simultaneously.

Under the conditions of using 30 m DEM and NewFlood two-dimensional hydrodynamic model Settings, this study compared the water flow directions of two flood-prone points in the scenarios of 2006 and 2020. The results showed that the differences in water flow patterns simulated in the two periods were not significant, indicating that under the current resolution and modeling framework, The undulation of the terrain has an important influence on the direction of local water flow. Flood-prone points 7 and 8 are located in the surrounding low-lying areas. Although the digital elevation model data shows that their altitudes are relatively low, there are differences in topographic features: low-lying terrain is prone to accumulate rainwater and accelerate water flow, thereby increasing the risk of flooding.

The research results show that there are significant inter-group differences in the impact of land use change on the peak flow velocity. Based on the statistics of the 8 typical point groups in Table 4, the mean change in the maximum flow velocity of the unchanged group (n = 4) was only 0.001 m/s, and the variation range could be ignored. The maximum flow velocity of the group of cropland converted to impervious (n = 4) increased by an average of 4.142 m/s, and the peak appearance time at some points was advanced. The flow field characteristics of the flood-prone area indicate that land use changes significantly affect the flow velocity, while the stable flow direction highlights the dominant role of topography. Low-lying areas are prone to water accumulation. Land use changes accelerate surface runoff and intensify the risk of floods. Urban planning should take into account land use, topographic features and drainage design to reduce the risk of urban flooding.

4. Discussion

4.1. Discussion on the Significance of This Study

In the rapid process of global urbanization, the impact of impermeable surface expansion on urban flooding has become a major global issue [1,2]. Existing studies have confirmed that there is a significant correlation between land use change and urban waterlogging [3,15]. However, methodological differences significantly influence the assessment of these impacts. Commonly used hydrological models, such as the SCS-CN method [7], primarily focus on the estimation of total runoff volume based on static land cover parameters. While effective for calculating cumulative water quantity, the SCS-CN method lacks the capability to simulate the spatial and temporal response of floodwaters. It cannot capture the dynamic propagation of flood waves or the spatial heterogeneity of flow velocities in complex urban terrain [30]. In contrast, this study utilizes the NewFlood two-dimensional hydrodynamic model. The NewFlood model solves the shallow water equations to explicitly simulate the physical flow process. This allows for a precise characterization of key dynamic parameters, such as the instantaneous velocity field and the temporal progression of water depth. This study uses NewFlood two-dimensional hydrodynamic model to simulate and compare the flood changes in the main urban areas of Wuhan in 2006 and 2020, focusing on the impact of land use change on the dynamic characteristics of urban flood, in order to fill the relevant research gap. The study found that land use change not only expanded the flood area and depth, but also significantly accelerated the arrival speed of flood peak and shortened the arrival time of flood peak by reducing the surface roughness. This conclusion emphasizes that in urban planning and flood control emergency management, equal attention should be paid to the dynamic process of floods, rather than just the flood volume. Furthermore, these findings suggest that the influence of urbanization on urban flooding is not uniform; rather, it appears to exhibit spatial and temporal variability associated with the direction of urban expansion.

4.2. Discussion on Comparing with Existing Study Results

Firstly, this study found that urbanization increased flood risk, which is consistent with the conclusions of many existing studies [28,31,32]. Secondly, the research further analyzes the hydrodynamic mechanisms driving these changes. Land use change affects the rainwater runoff confluence process and its dynamic response by altering the hydrodynamic parameters of the underlying surface. Specifically, when cultivated land or water areas transform into impermeable water surfaces, the underlying surface changes from a relatively rough and storable surface type to a smoother and hardened surface type. The reduction in its equivalent roughness will weaken the surface's blocking effect on runoff, thereby making it easier for surface runoff to form continuous confluence and accelerating the confluence process. While this phenomenon aligns with established hydraulic principles and previous literature regarding surface roughness and flow resistance [20,21], this study provides critical quantitative evidence specific to Wuhan's rapid urbanization. The value of this finding lies not merely in confirming the physical mechanism, but in quantifying its impact on urban safety margins. Specifically, the simulation reveals that land use transformation caused the peak flow time to advance by several minutes in specific flood-prone areas (e.g., Points 5 and 8). This quantification is crucial for defining precise time limits for early warning and response. The increase in flow velocity significantly raises the risk of instability for pedestrians and vehicles [29], while the shortened emergency response window intensifies the complexity of disaster reduction work. Thus, these quantitative results provide the necessary data support to transition from general qualitative warnings to precise, time-sensitive emergency protocols.

4.3. Practical Implications for Urban Flood Management

The greater significance of this study lies in its practical guiding value for urban stormwater and flood management. Based on the analysis of land use changes and hydrodynamic responses, we propose the following strategies to support Wuhan's urban planning and "Sponge City" construction: Targeted Land Use Optimization: Given the study's finding that the conversion of cropland and water bodies to impervious surfaces is the primary driver of increased flood risk, strict "Red Line" protection policies must be enforced. We recommend delimiting rigid protection zones around key lakes in Wuchang and Hongshan to preserve natural storage capacity. In new urban districts, the ratio of impervious surfaces should be strictly controlled, and green infrastructure (e.g., sunken green belts, rain gardens) should be mandated to compensate for the loss of natural infiltration and roughness. Risk prevention in Flood-Prone Areas: For identified high-risk points where flow velocity has increased significantly (e.g., Points 4 and 7), infrastructure layout should be adjusted. Critical facilities such as hospitals, schools, and power substations should avoid these high-velocity flow paths. Additionally, engineering measures such as increasing surface roughness via permeable pavements or adding deceleration baffles in drainage channels could be implemented to reduce flow velocity. Optimization of Emergency Response: The simulation indicates that urbanization shifts the flood peak time earlier. Consequently, the traditional emergency response time windows, which may be based on historical data, needs to be updated. We recommend that flood control agencies update their emergency plans to trigger warnings earlier during intense rainfall events, accounting for the "acceleration effect" caused by recent land use changes.

4.4. Limitations and Prospects

This study has certain limitations. The simulation analysis only covers natural flood scenarios and does not incorporate the human impacts of urban drainage networks. In actual heavy rainfall events, the drainage system clears part of the runoff, which reduces

the flood impact to some extent. Therefore, the simulation results cannot be completely equivalent to the actual observed water depth. Future research can further introduce variables such as population growth, construction intensity, planning control and engineering intervention on this basis, couple the NewFlood model with the urban drainage network model, and conduct a more systematic analysis of the driving process of land use change and its relationship with flood risk. In addition, there is still a certain degree of uncertainty regarding the differences and flow field characteristics of the land use change group in this study. On the one hand, the roughness parameter is assigned by land use type and homogenized within the same category, which may underestimate the spatial heterogeneity of internal roughness and water-blocking conditions in the built-up area. On the other hand, the statistics of the land use change group are based on 8 typical flood-prone points. In the future, the number of sample points still needs to be expanded to further enhance the robustness of the research results. Furthermore, introducing higher-precision micro-terrain data and the distribution characteristics of sponge city facilities can deepen the understanding of micro-scale processes and further optimize urban flood control design schemes. Finally, a crucial direction for future work is the integration of climate change projections. By incorporating results from Regional Climate Models (RCMs) into the extreme rainfall scenarios, future studies can simulate the impact of climate change induced intensification of rainfall on urban flooding. This will provide a more comprehensive and forward-looking scientific basis for long-term urban flood risk management and adaptation strategies.

5. Conclusions

(1) From 2006 to 2020, significant changes occurred in land use in the MUAW area, mainly manifested as a substantial expansion of impermeable area and a sharp reduction in cultivated land area. The proportion of impermeable urban area rose from 31.28% to 43.06%, among which the conversion of cropland to construction land contributed an increase of as high as 78.69%. The continuous reduction in water area highlights the necessity of constantly strengthening the protection of lakes.

(2) Under the conditions of different rainfall recurrence periods, the area within the urban region where land use change leads to an increase in water depth expands rapidly in the initial stage and reaches the maximum value at the peak of rainfall intensity before stabilizing. The distribution pattern of areas with increased water depth is highly consistent with the direction of urban expansion. Urbanization significantly accelerates the rate of runoff and intensifies local water accumulation by increasing impermeable area and reducing surface roughness, leading to a spatio-temporal dependence of urban flood risks on urban expansion and changes in rainfall intensity.

(3) Analysis of water depth, flow velocity changes and flow field characteristics in flood-prone areas shows that the transformation of land use types (from cropland or water bodies to impervious) significantly reduces surface roughness and accelerates stormwater runoff, resulting in an increase in peak flow velocity or earlier appearance of flood peaks in flood-prone areas—although topographic factors dominate the flow direction.

(4) From the perspective of planning practice, the control of the transformation of impervious water surfaces is the key to reducing the risk of urban flooding. This study puts forward strategies to support the urban planning and "sponge city" construction of Wuhan City. Important directions for the collaborative design of land use planning and flood control and disaster reduction have been proposed from aspects such as land use optimization, nature-based solutions and green infrastructure planning, risk prevention in flood-prone areas, and optimization of emergency response.

Author Contributions: Conceptualization, T.W. and Y.W.; methodology, T.W. and Y.W.; software, Y.W.; validation, T.W.; data curation, T.W.; writing—original draft preparation, T.W. and Y.W.; writing—review and editing, T.W. All authors have read and agreed to the published version of the manuscript.

Funding: This work was supported by the National Key Research and Development Program of China (No. 2023YFC3206604).

Data Availability Statement: The original data involved in this study have all been provided in the main text. For further information, please contact the corresponding author.

Conflicts of Interest: The research was conducted in the absence of any commercial or financial relationships that could be construed as a potential conflict of interest.

Abbreviations

The following abbreviations are used in this manuscript:

MUAW Main Urban Area of Wuhan

References

1. Rentschler, J.; Avner, P.; Marconcini, M.; Su, R.; Strano, E.; Vousdoukas, M.; Hallegatte, S. Global evidence of rapid urban growth in flood zones since 1985. *Nature* **2023**, *622*, 87–92. [CrossRef] [PubMed]
2. Balaian, S.K.; Sanders, B.F.; Abdolhosseini Qomi, M.J. How urban form impacts flooding. *Nat. Commun.* **2024**, *15*, 6911. [CrossRef] [PubMed]
3. Huang, S.; Gan, Y.; Chen, N.; Wang, C.; Zhang, X.; Li, C.; Horton, D.E. Urbanization enhances channel and surface runoff: A quantitative analysis using both physical and empirical models over the Yangtze River basin. *J. Hydrol.* **2024**, *635*, 131194. [CrossRef]
4. Haslinger, K.; Breinl, K.; Pavlin, L.; Pistotnik, G.; Bertola, M.; Olefs, M.; Greilinger, M.; Schöner, W.; Blöschl, G. Increasing hourly heavy rainfall in Austria reflected in flood changes. *Nature* **2025**, *639*, 667–672. [CrossRef] [PubMed]
5. Zhou, S.; Geng, X.; Jia, W.; Xu, H.; Xu, X.; Chen, H.; Wang, M.; Wu, Z. Towards climate-adaptive equality in coastal megacities: Assessing urban flooding risk disparities and nonlinear effect of multidimensional indicators through an interpretable LightGBM-SHAP framework. *Sustain. Cities Soc.* **2025**, *132*, 106809. [CrossRef]
6. Zeng, Z.J. Urban Waterlogging Simulation and LID Optimization Based on SWMM and FVCOM Coupling Model. Master's Thesis, Chongqing Jiaotong University, Chongqing, China, 2024.
7. Ma, L.J.; Wang, C.T.; Wang, W.J.; Zhang, L.L.; Huang, H.P.; Zhang, S.T. Regional runoff characteristics in Zhengzhou City based on SCS-CN model. *Bull. Soil Water Conserv.* **2022**, *42*, 203–209. [CrossRef]
8. Zhao, X.; Huang, G. Urban watershed ecosystem health assessment and ecological management zoning based on landscape pattern and SWMM simulation: A case study of Yangmei River Basin. *Environ. Impact Assess. Rev.* **2022**, *95*, 106794. [CrossRef]
9. Sun, N. Urban Waterlogging Numerical Simulation and Multi-Scale Risk Assessment. Master's Thesis, Shandong University of Technology, Zibo, China, 2024.
10. Yan, H.H.; Lu, Q.H. Application of MIKE FLOOD model in drainage schemes for high-density built-up areas: Taking the southern region of Fuhai River in Shenzhen as an example. *Pearl River* **2024**, *45*, 30–38. [CrossRef]
11. Wu, X.P.; Zhang, Y.; Ji, R.B. Application of XPSWMM hydraulic model in urban waterlogging control project of Pujiang County. *Munic. Eng. Technol.* **2025**, *43*, 189–196. [CrossRef]
12. Pelorosso, R.; Petroselli, A.; Cappelli, F.; Noto, S.; Tauro, F.; Apollonio, C.; Grimaldi, S. Blue-green roofs as nature-based solutions for urban areas: Hydrological performance and climatic index analyses. *Environ. Sci. Pollut. Res.* **2024**, *31*, 5973–5988. [CrossRef]
13. Bao, S.J. Research on the Identification of Recreational Hotspots and Visual Landscape Optimization of Waterfront Greenways in Wuhan Based on Multisource Data. Master's Thesis, Huazhong Agricultural University, Wuhan, China, 2023.
14. Jiang, Y.; Li, H.J.; Cheng, G. Evaluation of the planning and implementation of sponge city construction based on source control in Wuhan. *China Water Wastewater* **2023**, *39*, 44–48. [CrossRef]
15. Fu, M.; Jiao, L.; Su, J. Urban land system change: Spatial heterogeneity and driving factors of land use intensity in Wuhan, China. *Habitat Int.* **2025**, *159*, 103380. [CrossRef]
16. Liu, J.; Shi, Z. Quantifying land-use change impacts on the dynamic evolution of flood vulnerability. *Land Use Policy* **2017**, *65*, 198–210. [CrossRef]
17. Jiang, Y.; Zevenbergen, C.; Ma, Y. Urban pluvial flooding and stormwater management: A contemporary review of China's challenges and "sponge cities" strategy. *Environ. Sci. Policy* **2018**, *80*, 132–143. [CrossRef]

18. Wang, Y.; Liang, Q.; Kesserwani, G.; Hall, J.W. A 2D shallow flow model for practical dam-break simulations. *J. Hydraul. Res.* **2011**, *49*, 307–316. [CrossRef]
19. Zhou, Y.; She, D.; Wang, Y.; Xia, J.; Zhang, Y. Evaluating the impact of low impact development practices on the urban flooding over a humid region of China. *JAWRA J. Am. Water Resour. Assoc.* **2022**, *58*, 1264–1278. [CrossRef]
20. Yu, D.; Coulthard, T.J. Evaluating the importance of catchment hydrological parameters for urban surface water flood modelling using a simple hydro-inundation model. *J. Hydrol.* **2015**, *524*, 385–400. [CrossRef]
21. Lan, J.Y. Urban Land Use Change and the Response of Flood Disasters—Based on the Empirical Research of Nanjing, Wuhan and Hefei. Master's Thesis, Huazhong University of Science and Technology, Wuhan, China, 2021.
22. Liang, D.; Lin, B.; Falconer, R.A. A boundary-fitted numerical model for flood routing with shock-capturing capability. *J. Hydrol.* **2007**, *332*, 477–486. [CrossRef]
23. Guo, H.Q.; Han, Y.Z.; Bai, X.M. Hydrological effects of littet on different forest stands and study about surface roughness coefficient. *J. Soil Water Conserv.* **2010**, *24*, 179–183. [CrossRef]
24. Cui, X.P.; Guo, Y.X. Analysis on the spatio-temporal dynamic evolution of land use structure of western urban agglomerations in the past 40 years. *J. Arid. Land Resour. Environ.* **2022**, *36*, 16–24. [CrossRef]
25. Zhao, Y.; Zhang, Y.F.; Bu, X.; Li, Y.F.; He, Z.F. Land use change and its impact on ecosystem service value in Xinjiang from 2000 to 2020. *J. Tianjin Norm. Univ. Sci. Ed.* **2023**, *43*, 53–60. [CrossRef]
26. Pelorosso, R.; Apollonio, C.; Rocchini, D.; Petroselli, A. Effects of Land Use-Land Cover Thematic Resolution on Environmental Evaluations. *Remote Sens.* **2021**, *13*, 1232. [CrossRef]
27. Yang, X.; Chen, H.; Wang, Y.; Xu, C.-Y. Evaluation of the effect of land use/cover change on flood characteristics using an integrated approach coupling land and flood analysis. *Hydrol. Res.* **2016**, *47*, 1161–1171. [CrossRef]
28. Geng, Y.; Huang, X.; Hu, X.; Zhong, Y.; Liu, P. Urban flooding risk assessment based on the impact of land cover spatiotemporal characteristics with hydrodynamic simulation. *Stoch. Environ. Res. Risk Assess.* **2024**, *38*, 4131–4150. [CrossRef]
29. Wang, J.; Li, N. Review on flood hazard assessment index and grade classification. *China Flood Drought Manag.* **2019**, *29*, 21–26. [CrossRef]
30. Sun, Y.L.; Li, J.C.; Yang, D.; Bai, G.G.; Guo, K.H. Impact of land use change on catchment stormwater flooding process based on a hydrodynamic model. *J. Water Resour. Water Eng.* **2020**, *31*, 36–40. [CrossRef]
31. Feng, B.; Zhang, Y.; Bourke, R. Urbanization impacts on flood risks based on urban growth data and coupled flood models. *Nat. Hazards* **2021**, *106*, 613–627. [CrossRef]
32. Lei, Y.; Cao, H.; Zhou, X.; Mills, J.; Xiao, W. Impact of land use/land cover changes on urban flooding: A case study of the Greater Bay Area, China. *IEEE J. Sel. Top. Appl. Earth Obs. Remote Sens.* **2024**, *17*, 13261–13275. [CrossRef]

Disclaimer/Publisher's Note: The statements, opinions and data contained in all publications are solely those of the individual author(s) and contributor(s) and not of MDPI and/or the editor(s). MDPI and/or the editor(s) disclaim responsibility for any injury to people or property resulting from any ideas, methods, instructions or products referred to in the content.